An Analytic Model for Estimating the Length of the Velocity Saturated Region in GaAs MESFET's

Curtis Leifso, *Student Member, IEEE,* and James W. Haslett, *Senior Member, IEEE*

***Abstract*—An analytical model is presented for estimating the length of the portion of a FET channel with velocity saturated carriers. The model is based on previous work proposed by Pucel *et al.* [1], [2], and has been adapted to remove discontinuities between extreme bias conditions. The need for complicated numerical solutions has also been removed making the model suitable for use with circuit simulators. Results obtained from the model agree well with previously proposed models over a wide range of bias conditions where velocity saturation can be either dominant or negligible, depending on the overall channel length and bias conditions.**

***Index Terms*—Gallium arsenide, MESFET, modeling, velocity saturation.**

I. Introduction

KNOWLEDGE of the length of the velocity saturated region (LVSR) of a FET channel aids in modeling both the dc and noise performance of GaAs MESFET's. For devices with gate lengths less than 0.5 μm, most of the channel is velocity saturated, and it is the saturation velocity that is of interest [3], [4]. Devices with gate lengths larger than this are still commonly used, however, and the effects of velocity saturation can vary with the biasing conditions.

Much attention has been given to modeling the LVSR in MOSFET's [5]–[7]. However, these works cannot be directly applied to MESFET's due to the fundamentally different physical mechanisms causing current and velocity saturation in these devices [8].

An analytic model for estimating the LVSR has been presented by Pucel *et al.* for the GaAs MESFET for use in a noise model presented in the same paper [1], [2]. The derivation presented was an extension of earlier work done by van der Ziel [9], [10] on the development of commonly known FET noise models. Pucel *et al.*extended the analysis to include the effects of the velocity saturated region by utilizing the current continuity in the channel at the point where velocity saturation occurs. This model is limited in that it is not continuous over all valid bias conditions and requires extensive boundary condition checks. The model also lacks an explicit form for the LVSR and requires difficult numerical solution of sensitive functions. Both of these shortcomings make this model unsuitable for implementation in circuit simulators or for readily obtaining practical estimates of the LVSR.

Manuscript received April 14, 1999. This work was supported by the Natural Sciences and Engineering Research Council of Canada under Grant OGP0007776. The review of this paper was arranged by Editor M. F. Chang.

The authors are with TR Labs and the Department of Electrical and Computer Engineering, University of Calgary, Calgary, Alta., Canada T2N 1N4 (e-mail: haslett@enel.ucalgary.ca).

Publisher Item Identifier S 0018-9383(00)03396-7.

This model has been experimentally confirmed by Folkes [11] who pointed out that the model is not practical to implement in circuit simulators since calculation of the LVSR is too complicated. Using a different method presented by Shur [12], Onodipe and Guvench in more recent work rederived the same numerical model for the LVSR as given by Pucel *et al.* [13]. This model was again experimentally confirmed by Onodipe and Guvench for numerous bias conditions.

In this paper, a variation of the Pucel–Statz–Haus model is presented, which depends explicitly on the total channel length L, Shockley pinch-off potential W_{oo}, drain to source voltage V_{ds} and the source to gate voltage V_{sg}, eliminating the need for difficult numerical solutions. The model is also self limiting in that the result is valid for all possible bias conditions and does not need to be checked against the overall channel length, L, as the LVSR approaches L.

For the model developed, the LVSR has the same functional dependence on V_{ds} as a recent CMOS model developed by Wong and Poon [5]. The LVSR dependence on the overall channel length, however, is significantly different in these two devices.

II. Overview of the Pucel–Statz–Haus Model

In notable early work in noise analysis of MESFET's, van der Ziel presented a dc model based on physical principles of the device operation [9], [10]. In this model and several other variations proposed [14], it was assumed that the effects of the velocity saturated region were negligible and confined to a small fraction of the channel near the drain end.

For devices with a channel length much greater than 1 μm, this assumption is generally valid for practical bias conditions. As the channel length is decreased, the LVSR can occupy most of the overall channel length, depending on the bias conditions, making this assumption invalid. In a later analysis proposed by Pucel *et al.* [1], [2] the original van der Ziel thermal noise analysis was modified to include noise contributions from the velocity saturated region.

Straightforward manipulation of the drain current expression given by van der Ziel *et al.* showed that with both velocity saturated and constant mobility channel sections, the dc bias conditions of the FET could be characterized by six equations given by

$$I_d = g_o W E_{sat}(1-p) \tag{1}$$

$$V_{ds} = W_{oo}\cdot(p^2-s^2)+\left(\frac{2aE_{sat}}{\pi}\right)\cdot\sinh\left(\frac{\pi}{2a}\mathrm{LVSR}\right) \tag{2}$$

$$s = \sqrt{\frac{V_{sg}+\phi}{W_{oo}}} \tag{3}$$

0018-9383/00$10.00 © 2000 IEEE

$$L_1 = \frac{f_1(p,\, s)W_{oo}}{E_{sat}(1-p)} = L - \text{LVSR} \tag{4}$$

$$p = \sqrt{\frac{V_{sg} - V_p + \phi}{W_{oo}}} \tag{5}$$

$$d = \sqrt{\frac{V_{ds} + V_{sg} + \phi}{W_{oo}}} \tag{6}$$

where

L_1	length of constant mobility region;
V_p	channel voltage at the pinch off point;
W_{oo}	Shockley pinch off potential; [15]
g_o	channel conductivity $= \mu_o N_D q a$;
a	undepleted channel depth;
μ_o	constant carrier mobility;
$f_1(p,\, s)$	$= p^2 - s^2 - (2/3)(p^3 - s^3)$;
L	overall channel length;
N_D	doping density;
E_{sat}	E-field at the pinch off point;
ϕ	reverse bias Schottky junction voltage;
$p,\, s,\, d$	normalized gate referred channel potentials at the pinch off point, source, and drain, respectively.

A common set of assumptions were made in this derivation and are briefly summarized. As shown in Fig. 1, it is assumed that at the pinch off point $x = L_1, E = E_{sat}$ and the normalized gate referred channel potential p is given by (5). For all $x \leq L_1$ the mobility is assumed to be constant and the carrier drift velocity increases linearly with the E-field in the channel. For all $x > L_1$, the mobility decreases with increasing E-field and the carrier velocity is saturated at a constant value.

The above model described by (1)–(6) is valid when both regions exist in the channel and (4) gives a value for L_1 between 0 and L μm. As the channel length is increased, the normalized potential p increases until (4) indicates $L_1 > L$. From this, these equations can only be used provided a conditional check is included to limit the value of L_1 and hence the calculated LVSR. This can be complicated when implementing the model in a circuit simulator since an upper limit exists on both p as well as the normalized drain potential d given by (6), where p cannot exceed d. When modeling components whose values must be determined from equations in a simulator such as Libra, conditional expressions are not easily included.

A lower limit also exists on p, since the condition $s < p < P_u$ must be maintained, where P_u is the upper limit on p given by the smallest of either d or the value of p that makes $L_1 = L$ as calculated by (4). Calculation of p can be easily done using (1) for a given bias current, however, simulations are more conveniently done when p is obtained from (2) and (3) using a known V_{ds} and V_{sg}. This is more useful in dc modeling where the dc drain current is typically the desired quantity to model.

Determining V_{sg} and V_{ds} is easily done in most simulators, however, the LVSR cannot be found explicitly since p must be found from numerical solution of an extremely sensitive function in (2). If the channel potential at the pinch off point was known, (5) could be used to calculate p. This quantity must be found from solution of the remaining five equations and serves only to define the variable p.

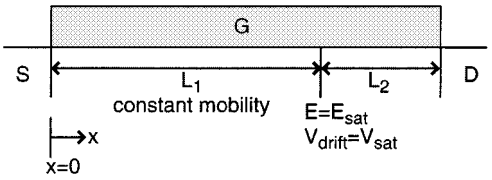

Fig. 1. Assumed E-field distribution in the channel.

From this, two modifications to the model must be made if it is to be conveniently used in a circuit simulator. First, the LVSR must be an explicit function of V_{sg} and V_{ds} eliminating the need for numerical solution. Secondly, the final expression for the LVSR must be self limiting, i.e., it must vary between zero and L for all bias conditions that keep the device in saturation.

III. Development of Alternative Model

A. Explicit Form of LVSR

In order to get the LVSR as a function of V_{ds}, p must be found as an explicit function of V_{ds}. Solving for the LVSR in (2), substituting the resulting expression into (4) and using the identity

$$\sinh^{-1}(x) = \ln\left(x + \sqrt{1+x^2}\right) \tag{7}$$

a new function $x(p)$ can be defined as

$$x(p) = \frac{2a}{\pi}\ln\left(y + \sqrt{1+y^2}\right) + \frac{f_1(p,\, s)W_{oo}}{E_{sat}(1-p)} - L = 0 \tag{8}$$

whose roots give the required value of p. The dimensionless quantity y is defined as

$$y(V_{ds},\, p) = \frac{\pi}{2aE_{sat}}(V_{ds} - W_{oo}(p^2 - s^2)). \tag{9}$$

For devices with channel lengths < 1 μm $p \approx s$ and y can be considered to be $\gg 1$ provided V_{ds} is large enough to keep the device in saturation. As L increases, p increases which slightly lowers $y(V_{ds},\, p)$. However, for most practical device geometries and bias conditions, the assumption $y(V_{ds},\, p) \gg 1$ is valid and hence (8) reduces to

$$x(p) \approx \frac{2a}{\pi}\ln(2y(V_{ds},\, p)) + \frac{f_1(p,\, s)W_{oo}}{E_{sat}(1-p)} - L = 0 \tag{10}$$

which must be solved for p. A plot of this function over a range of p values where $s < p < 1$ is shown in Fig. 2 for a wide range of channel lengths.

The large increase in the slope of $x(p)$ for large p values occurs when s is small (V_{sg} is low), d is large (V_{ds} is large) and the overall channel length is much larger than 2 μm. In practical circuits, especially microwave designs, these conditions rarely occur. Instead submicron processes are preferred with minimal bias voltages.

These conditions result in the LVSR occupying a large fraction of the channel which causes p to be slightly larger than s for a wide range of bias conditions. This makes it possible to approximate $x(p)$ with a local series expansion over a bounded region just before the slope of $x(p)$ increases rapidly, as opposed to a global series expansion about some arbitrary point that is not

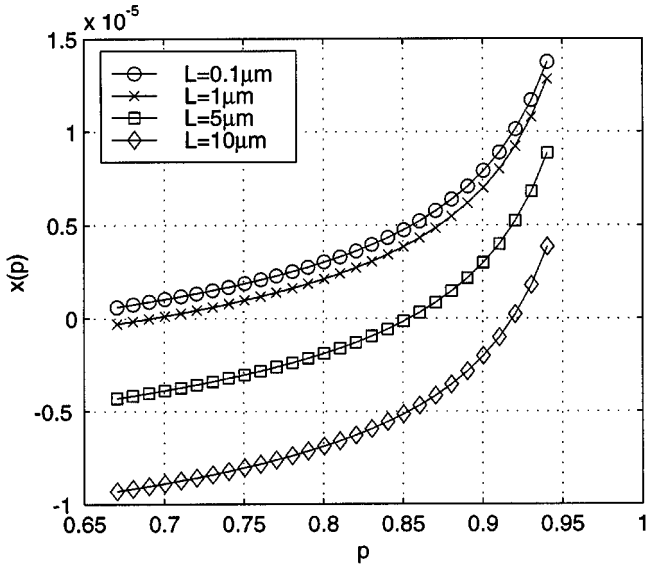

Fig. 2. Dependence of $x(p)$ on p and L from the original Pucel *et al.* model.

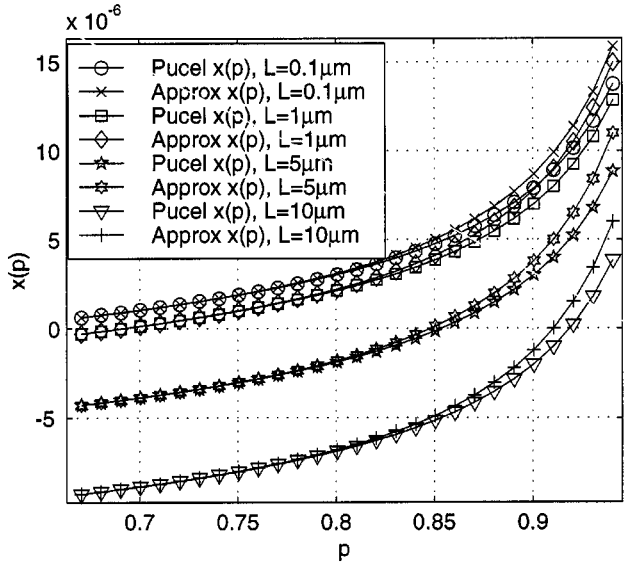

Fig. 3. Plot of $x(p)$ from Pucel *et al.*model with the approximation $\tilde{x}(p)$ as p is varied.

easily determined if the model is to be valid for a wide range of channel lengths.

For a small local region, a common quadratic approximation to a function given in most numerical methods texts, (Powell [16]) is

$$x(p) \approx \tilde{x}(p) = x(P_L) + x'(P_L)(p - P_L) + \left[\left(\frac{3[x(P_U) - x(P_L)]}{(P_U - P_L)^2}\right) - \left(\frac{2x'(P_L) + x'(P_U)}{(P_U - P_L)}\right)\right](p - P_L)^2 \quad (11)$$

where $x'(p)$ is found by differentiating (10) to get

$$x'(p) \approx \left(\frac{W_{oo}}{E_{sat}}\right)\left(\frac{2p(1-p)^2 + f_1(p, s)}{(1-p)^2}\right). \quad (12)$$

A good choice for the lower limit of the expansion interval is clearly when $p = s$. In order to choose the upper limit of the interval, (4) can be solved for the point at which the entire channel can be modeled with constant mobility or $L_1 = L$, which requires solution of a cubic equation in p. When the expansion is done within these limits, the portion of $x(p)$ with large slope is not modeled as well, which reduces the model's accuracy as p gets larger (corresponding to long channel lengths). This gives an approximation to $x(p)$ that will be valid for all practical operating conditions and FET channel lengths for reasonably low L (below 2 μm).

A better approximation for all channel lengths can be obtained with straightforward manipulation of the original $x(p)$ expression in (10) and noting that the logarithmic term changes much slower than $f_1(p, s)$ as p is increased. Rewriting (10) as

$$x(p) = \frac{\frac{2aE_{sat}(1-p)}{\pi}\ln(2y) + f_1(p, s)W_{oo} - LE_{sat}(1-p)}{E_{sat}(1-p)} \quad (13)$$

will give a quadratic solution to p provided a quadratic approximation to $f_1(p, s)$ and a linear approximation of $\ln(2y(V_{ds}, p))$ can be reasonably made. Using the approximation method given in (11), $f_1(p, s)$ and $\ln(2y(V_{ds}, p))$ can be expanded as quadratic and linear functions given by

$$f_1(p, s) \approx 2s(1-s)(p-s) + \left[\frac{3f_1(P_U, s)}{(P_U - s)} - 4s(1-s) - 2P_U(1-P_U)\right] \cdot \frac{(p-s)^2}{P_U - s} \quad (14)$$

and

$$\ln(2y) \approx \ln\left(\frac{\pi V_{ds}}{aE_{sat}}\right) - \left(\frac{2sW_{oo}}{V_{ds}}\right)(p - s) \quad (15)$$

respectively, where P_U is the upper limit on p derived in Section IV. Substituting these approximations into (13) and simplifying gives a quadratic $\tilde{x}(p)$ summarized in Section III-C that can be solved to give two roots, one of which will be greater than 1 and can be discarded.

Fig. 3 shows a plot of $x(p)$ calculated from the Pucel *et al.* model and the new approximation $\tilde{x}(p)$ over a range of p values when these two approximating functions for $f_1(p, s)$ and $\ln(2y)$ are used. The solution for p is found at the point where $\tilde{x}(p) = 0$. From the close agreement shown in Fig. 3 when $x(p)$ and $\tilde{x}(p)$ equal zero, it is clear that a quadratic estimate of $f_1(p, s)$ and a linear approximation to $\ln(2y(V_{ds}, p))$ can be reasonably made without compromising the accuracy of the overall function $\tilde{x}(p)$.

B. Self Limiting Modifications

Limiting the LVSR expression to $0\ \mu\text{m} < \text{LVSR} < L\ \mu\text{m}$ implies $\tilde{x}(p)$ has one zero in the open interval (s, P_U), where P_U is the upper limit on p such that $\tilde{x}(P_U) > 0$ and $P_U \leq d$. Since $x(p)$ is monotonically increasing in the interval (s, P_U)

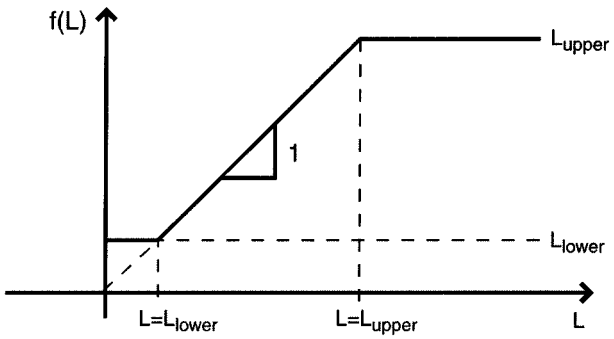

Fig. 4. Ideal function $f(L)$ for limiting $\tilde{x}(p)$.

the lower limit occurs when $p = s$ and thus $\tilde{x}(s)$ must be negative for the zero to exist.

As discussed, there are two possible upper limits on p from which the smallest must be chosen. First, solution of the cubic (4) when $L_1 = L$ gives a value of p, $\tilde{p}$ that would indicate no velocity saturation within the channel. This solution can take on any value between s and 1 and hence must be compared to d to determine the actual upper limit P_U.

By noting that $x(p) = (2a/\pi)\ln(2y)$ when $L_1 = L$, and using the identity given in (7) and the expression for s from (3), it is easy to show that d will always be greater than $\tilde{p}$ and hence $P_U = \tilde{p}$. $\tilde{p}$ is found from (4) when $L = L_1$ and is not bias dependent so it only needs to be calculated once for a given device geometry, and is given as

$$\tilde{P} = P_U = \sqrt{\frac{V_{ds} + V_{sg} + \theta - \frac{a}{\pi}E_{sat}}{W_{oo}}}$$

Knowing the upper and lower limits on p, several alternatives are available to limit $\tilde{x}(p)$ and hence the expression for the LVSR. The overall expression for the LVSR cannot be directly truncated when it approaches the valid limits since $x(p)$ has no zero within the range $s < p < P_U$ as shown in Fig. 3 for the case when $L = 0.1$ μm. To guarantee a zero in the required interval implies $\tilde{x}(s) < 0$ and $\tilde{x}(P_U) > 0$. This can be accomplished with several alternatives. The most flexible is substituting an expression for the channel length that limits L at set boundaries and leaves it unaltered when within a valid range. This makes the effect of the limiting function easier to see since $x(p)$ has a simple linear dependence on L according to (10).

In each case, a function is required whose value is the original argument until the argument approaches some boundary, beyond which an asymptotic limit is reached. Such an ideal function is shown in Fig. 4. Using the conditions $\tilde{x}(s) < 0$ and $\tilde{x}(P_U) > 0$ discussed, (10) can be rearranged to give the upper and lower limits on L, L_U and L_L as

$$L_L = \left(\frac{2a}{\pi}\right)\ln\left(\frac{V_{ds}\pi}{aE_{sat}}\right) \tag{16}$$

and

$$L_U = \left(\frac{2a}{\pi}\right)\ln(2y|_{(p=P_U)}) + L. \tag{17}$$

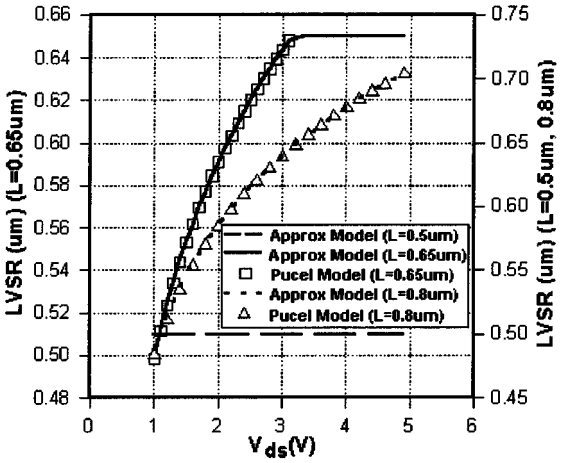

Fig. 5. LVSR predicted by Pucel *et al.* model and new model for different V_{ds} conditions. When $L = 0.5$ μm and for part of the $L = 0.8$ μm curves the Pucel model does not have a valid solution.

In order to position the curve of Fig. 4 as required, the function must be modified to be of the form

$$f(L) = Lu(L - L_L) + (L_U - L)u(L - L_U) + L_L u(L_L - L) \tag{18}$$

where u is the unit step function.

C. New Model Summary

The complete explicit model for the LVSR is given as

$$\text{LVSR} = L - \frac{(p^2 - s^2 - \frac{2}{3}(p^3 - s^3))W_{oo}}{E_{sat}(1-p)} \tag{19}$$

where p is the smallest root of the quadratic $Ap^2 + Bp + C = 0$ whose coefficients are

$$\begin{aligned} A =& \frac{W_{oo}C_{21}\pi V_{ds} + 4aE_{sat}sW_{oo}}{\pi V_{ds}} \\ B =& 2sW_{oo}(1-s) - 2sC_{21}W_{oo} + f(L)E_{sat} \\ & - \frac{2}{\pi}aE_{sat}\ln\left(\frac{\pi V_{ds}}{aE_{sat}}\right) - \frac{4aW_{oo}sE_{sat}(1+s)}{\pi V_{ds}} \\ C =& \frac{2}{\pi}aE_{sat}\ln\left(\frac{\pi V_{ds}}{aE_{sat}}\right) + \frac{4aW_{oo}s^2E_{sat}}{\pi V_{ds}} \\ & - 2s^2(1-s)W_{oo} - f(L)E_{sat} + s^2C_{21}W_{oo} \end{aligned}$$

and

$$\begin{aligned} C_{21} =& 3\frac{P_U^2 - s^2 - \frac{2}{3}(P_U^3 - s^3)}{(P_U - s)^2} \\ & - \frac{4s(1-s) + 2P_U(1-P_U)}{(P_U - s)}. \end{aligned}$$

IV. Model Performance

A. Comparison to Pucel–Statz–Haus Model

A comparison of the approximate function $\tilde{x}(p)$ with $x(p)$ from the Pucel model is shown in Fig. 3 for several different bias conditions. The most common measures of LVSR models are the dependence on V_{ds} and L. Fig. 5 shows these plots for several bias voltages and channel lengths. The actual LVSR es-

timates given by the Pucel model are also plotted in Fig. 5. These plots show excellent agreement between these two functions when both a velocity saturated and constant mobility region exist.

When L is made $\ll 1$ μm, most of the channel is velocity saturated and $p \approx s$. As shown in Fig. 5, the limiting function of L causes $\tilde{x}(p)$ to remain less than zero resulting in the LVSR to equal L as required. As shown when $L > 0.65$ μm V_{ds} can be gradually increased until the entire channel becomes velocity saturated. For gate lengths < 0.65 μm essentially the entire channel is velocity saturated when the device is biased in saturation. The Pucel *et al.* model is not valid in this region and has no solution.

Fig. 5 also shows the effects of the limiting function on the LVSR. From this, the effect of substituting $f(L)$ from (18) for L in $\tilde{x}(p)$ is to ensure that a zero exists in the valid interval for p thus causing the LVSR to limit at L when the channel length is small and V_{ds} is sufficiently large to velocity saturate the entire channel. Note that when s and d are calculated from (3), neither may exceed one. $s \geq 1$ occurs when the entire channel is pinched off and no current flows in the device. This does not need to be checked within the model since it is a condition that will be avoided in the circuit design and biasing of the device.

V. Conclusions

An analytic model to estimate the LVSR in a GaAs MESFET has been presented. The model is continuous between conditions where velocity saturation can be either dominant or negligible. The calculated LVSR is given explicitly as a function of simple process parameters and does not require numerical solution, thus making the model suitable for use in circuit simulators. The results obtained from the model agree well with those obtained from more difficult numerical solution of the Pucel–Statz–Haus model on which it is based.

Acknowledgment

The authors would like to thank TR Labs and the Canadian Microelectronics Corporation.

References

[1] H. Statz, H. A. Haus, and R. A. Pucel, "Noise characteristics of gallium arsenide field-effect transistors," *IEEE Trans. Electron Devices*, vol. ED-21, pp. 549–562, Sept. 1974.

[2] ——, "Signal and noise properties of gallium arsenide microwave field-effect transistors," *Adv. Electron. Electron Phys.*, vol. 38, pp. 195–263, 1975.

[3] P. M. Smith, M. Inoue, and J. Frey, "Electron velocity in Si and GaAs at very high electric fields," *Appl. Phys. Lett.*, vol. 37, pp. 797–798, 1980.

[4] C. S. Chang and H. R. Fetterman, "Electron drift velocity versus electric field in GaAs," *Solid-State Electron.*, vol. 29, pp. 1295–1296, 1986.

[5] H. Wong and M. C. Poon, "Approximation of the length of velocity saturation region in MOSFET's," *IEEE Trans. Electron Devices*, vol. 44, pp. 2033–2036, Nov. 1997.

[6] H. Wong, "A physically-based MOS transistor avalanche breakdown model," *IEEE Trans. Electron Devices*, vol. 42, pp. 2197–2202, Dec. 1995.

[7] N. D. Arora, R. Rios, R. C. Huang, and K. Raol, "PCIM: A physically based continuous short-channel IGFET model for circuit simulation," *IEEE Trans. Electron Devices*, vol. 41, pp. 988–987, June 1994.

[8] P. H. Ladbrooke, *MMIC Design—GaAs FET's and HEMT's*. Boston, MA: Artech House, 1989.

[9] A. van der Ziel, "Noise resistance of FET's in the hot electron regime," *Solid-State Electron.*, vol. 14, pp. 347–350, Apr. 1971.

[10] ——, "Thermal noise in field-effect transistors," *Proc. IRE*, vol. 50, pp. 1808–1812, 1972.

[11] P. A. Folkes, "Thermal noise measurements in GaAs MESFET's," *IEEE Electron Device Lett.*, vol. 6, Dec. 1985.

[12] M. Shur, *GaAs Devices And Circuits*. Englewood Cliffs, NJ: Prentice-Hall, 1987.

[13] B. O. Onodipe and M. G. Guvench, "Transverse magnetic field effects on GaAs MESFET's: Analytical model and experiments," in *Proc. 8th IEEE Bienn. Univ./Gov./Indust. Symp.*, 1989.

[14] W. Baechtold, "Noise behavior of GaAs field-effect transistors with short gate lengths," *IEEE Trans. Electron Devices*, vol. ED-19, pp. 674–680, May 1972.

[15] W. Shockley, "A unipolar field-effect transistor," *Proc. IRE*, vol. 40, pp. 1365–1376, Nov. 1952.

[16] M. J. D. Powell, *Approximation Theory and Methods*. Cambridge, U.K.: Cambridge Univ. Press.

Curtis Leifso (S'97) was born in Manitoba, Canada, on June 14, 1976. He received the B.Sc. degree in electrical engineering from the University of Calgary, Calgary, Alta., Canada, in 1997, where he is currently pursuing the Ph.D. degree in the same department.

His research is focused on MMIC design of active resonant circuits for use in microwave filtering applications.

James Haslett (S'64–M'66–SM'79) was born in Saskatchewan, Canad, on September 27, 1944. He received the B.Sc. degree in electrical engineering from the University of Saskatchewan, Saskatoon, Sask., Canada in 1966, and the M.Sc. and Ph.D. degrees from the University of Calgary, Calgary, Alta., Canada, in 1968 and 1970, respectively.

He then joined the Department of Electrical Engineering, University of Calgary, where he is currently a Professor. He was Head of the department from 1986 to 1997, and has been a Consultant to oilfield instrumentation firms for the past 25 years. His current research interests include analog and digital VLSI design, noise in semiconductor devices, high temperature electronics for instrumentation applications, and RF microelectronics for telecommunications.

Dr. Haslett is a Member of the Association of Professional Engineers, Geologists and Geophysicists of Alberta, the Canadian Astronomical Society, the Canadian Society of Exploration Geophysicists, and the American Society for Engineering Education.